

Supporting Information

Photovoltaic charge generation visualized at the nanoscale: a proof of principle

By Andrea Liscio, Giovanna De Luca, Fabian Nolde,
Vincenzo Palermo, Klaus Müllen, Paolo Samori

Experimental procedures

N,N'-bis(1-ethylpropyl)-3,4:9,10-perylene-bis(dicarboximide) (PDI)¹ and regioregular poly(3-hexylthiophene) P3HT (Aldrich, possessing $M_n = 18200$, $M_w = 45790$ as determined by gel permeation chromatography (GPC) analysis relative to polystyrene standards) have been deposited from solution by drop casting on silicon substrates covered by a few nm thick native oxide layer.

Films of neat PDI were prepared by applying a 10 μ L drop of a 0.53 mg/mL concentrated solution in CHCl_3 to SiO_x . Films of P3HT were obtained by applying a 10 μ l drop of a 7.5 mg/mL concentrated solution in CHCl_3 to the substrate. Films were left to dry in air.

The blend films have been prepared in a two step procedure using the same solutions and volumes applied to the surface during the preparation of the aforementioned neat films. First the PDI solution has been drop cast on SiO_x . After about 3 hours, the P3HT solution was applied on its top and the film was left to dry in air. The blend films have been prepared in atmosphere saturated with vapors of CHCl_3 , to slow down solvent evaporation and improve self assembling. The silicon substrate was cleaned prior to use with standard RCA procedure. In particular, the generation of the most interesting morphologies for our specific KPFM studies, i.e. featuring several clusters of PDI both in contact and isolated from the P3HT phase, were obtained in the presence of a small amount of paraffins dissolved into the solutions used for the deposition. The paraffins (brought into the system by a Parafilm M[®] tape used to seal the samples) lead to the formation of a thin apolar layer on the SiO_x , and ultimately improved the insulation of the organic nanostructures and thus photovoltage generation.

AFM combined with KPFM measurements have been performed at room temperature in a sealed chamber filled with N_2 (RH < 10%) with a commercial apparatus (Multimode IIIA - Veeco equipped with Extender Electronics module). Antimony (n) doped Silicon tips have been used. In order to obtain sufficiently large and detectable mechanical deflections, we employed soft ($k < 4$ N/m) cantilevers with oscillating frequencies in the range $60 < \omega < 100$ KHz (SCM, Veeco). Both sides of the cantilever were coated with 20 nm of Pt/Ir, with a buffer layer (3 nm) of Cr to improve the adhesion. To simultaneously acquire AFM and KPFM images, a topographic line scan is first recorded by AFM operating in Tapping Mode and then that same line is re-scanned in Lift Mode

with the tip raised to a lift height of about 30 nm. The basic principles of KPFM have been described in details elsewhere.² In brief, KPFM provides a local measure of the Surface Potential (SP) differences between conductive tip and the sample under investigation. SP is defined as: $(WF_{\text{tip}} - WF_{\text{sample}} - \Delta_{\text{pol}})/q$, where WF_{tip} and WF_{sample} are the work functions of tip and sample, Δ_{pol} is the polarization induced by the tip and q is the magnitude of the elementary charge. In the performed KPFM experiments, a bias voltage $V_{\text{tip}} = V_{\text{DC}} + V_{\text{AC}} \cdot \sin(\omega t)$ is applied directly to the tip, holding the sample to the ground potential; ω is the resonant frequency of the cantilever V_{DC} and V_{AC} are a continuous and alternate bias respectively. A feedback loop continually adjusts V_{DC} to nullify the force component at frequency ω between the tip and the sample. V_{DC} is recorded as a function of the position, yielding a map of the sample SP. The calibration and the optimization of the experimental parameters are achieved using the procedure proposed by Jacobs and co-workers.³

To produce the photogenerated charges, samples were illuminated with a white tungsten halogen lamp at a power of 61 mWcm^{-2} . The intensity of the incident light was measured with an Oriel thermopile. A significant variation of potential with light (due to the photovoltaic effect) was observed only for blends of the two materials and not on mono-component PDI films.

Measurements performed on various layers of mono-component PDI did not exhibit any change in potential under illumination, while thin films of P3HT showed only a small and uniform potential change with light.

Scanning Probe Microscopies are probe techniques that reveal local features, which are not necessarily representative for the whole sample surface. Because of this reason, it is appropriate to record and process several images on different points of the sample surface, making it possible to minimize the influence of a particular sample area and to determine an average behavior. All the evaluation have been carried out quantitatively and averaged over a large number of samples making use of two different image processing softwares: SPIP, and “Nanoscope” version 6.13R1 digital instruments Veeco. Widths measured with AFM have been corrected for tip broadening.⁴ For all values derived from AFM and KPFM data presented in this paper the error is evaluated as the standard deviation, as measured in many different measurements sessions.

Quantitative KPFM estimation of SPs

A previous work⁵ has shown that the measured SP of nano-objects having a lateral size (i.e. width) between a few tens and a few hundreds of nm features an apparent variation. This variation is due to the limit brought into play by the physical principle governing the KPFM imaging and consequently

also by the size of the probing KPFM tip. In KPFM measurement, the SP signal is averaged over an *effective area* of the sample surface interacting with the tip which, due to the long-range nature of the electrostatic tip-sample interactions, can be many tens of nm wide. Hence, for a size of the adsorbate nanostructure smaller than the effective area, both adsorbate and substrate potentials contribute to the SP measured in a given position on a surface. We have devised a semi-quantitative model which permits i) to estimate the effective area, ii) to calculate the effective SP of the adsorbate removing the component of the substrate potential and, in the case of flat adsorbate structures on flat substrate, iii) to simulate the KPFM image.

In the achieved experimental conditions, the effective area has been quantified amounting about to 100-150 nm. Figure S11a,b display the KPFM images of P3HT and PDI cast on SiO_x corresponding to the AFM topographic images shown in fig. 1c,d. The sizes of P3HT rhomboidal aggregates and PDI needles-like assemblies are both larger than the effective area. In this case, the potential component of substrate can be neglected. Differently, when the two molecules are blended together (as shown in Figure 2), the PDI aggregates in smaller clusters having size which vary from about 50 nm to few hundreds of nm. We therefore performed a quantitative analysis comparing the size of the PDI cluster with those of the effective area. We started considering the isolated PDI clusters (marked with I in Fig. 2) which possess i) size varying from 50 to 250 nm and ii) no SP variations inside the cluster due to the contact region with the P3HT island. The size-dependence of the measured SPs is reported in Figure S12. The data of the PDI clusters are grouped according to their size with a step of 50 nm. The reported values are measured during sample illumination (open red circles) and under dark (black squares). For PDI clusters having size smaller than 150 nm, the SP value decreases with the size of the object. The potential is underestimated, because this value is averaged with those of the substrate. When the size of the object under investigation is larger than 150 nm, the measured SP value is constant, featuring only small fluctuations within the experimental variance, and it corresponds to the asymptotic value. Hence, for our quantitative analysis we took into account in the statistic only the SP measured on PDI clusters larger than 150 nm.

In the figure S12, the SP values of the sample under or without illumination are displayed using two different shifted vertical axes (red and black, respectively) to align the two asymptotic SP values which amount to -32 ± 5 mV and -12 ± 4 mV, respectively. Moreover, the two data sets are reported using the same potential range (i.e. 25 mV). The good agreement between the two observed trends provides unambiguous evidence that the apparent SP variation is an experimental effect due to the size of the PDI clusters.

Moreover, a further dependence of the measured SP on the height of the adsorbed structure under study is observed. The correlation plot between the height of the PDI object and the corresponding SP value is displayed in figure SI3. Increasing the height of these objects, the measured SP varies from about -10 to -80 mV, with an error bar amounting to ± 5 . We can rule out the cross-talking between the topographic and potential signals suggesting that this effect can be ascribed (i) to the band bending of PDI when it is in contact with the SiO_x substrate and (ii) to the averaging of the SP signal due to the effective volume of the sample which interacts with the tip. The effective volume can be treated as a natural extension of the effective surface and it is due to the region of the sample underneath the surface interacting with the tip. This aspect will be discussed in detail elsewhere.⁶

The KPFM measurements performed on P3HT and P3HT:PDI blend are not affected by this problem because both the observed structures (i.e. rhomboidal and cluster ones) do not exhibit any appreciable variation in heights within the variance due to the noise level. In the blend, the height of the PDI clusters amounts to about 30 nm (vertical red line shown in fig. SI3). Hence, the corresponding SP value should be compared only with those of the structures with similar height found in monocomponent films. When the sample is not illuminated, a good agreement is observed between the SP of PDI cluster and those of needle-like assembly having same thickness, which amount to -14 ± 4 mV and -12 ± 4 mV with respects to the SP of the substrate, respectively. The SP value obtained from the KPFM measurements performed on the P3HT:PDI blend is displayed in Fig. SI2 by a horizontal red line. A summary of the measured SP dependence respect to the widths and the heights of the nanostructures is reported in Table SI1.

In order to take into account the effect of both vertical and horizontal nanostructure size on the measured SP, the potential values reported in Table 1 are calculated considering all the PDI clusters larger than the effective area and the PDI needle-like assemblies having the same height of the cluster (i.e. 30 nm).

Measured SP	P3HT	PDI	P3HT:PDI
Size-dependence	NO	YES	YES (only PDI)
Height-dependence	NO	YES	NO

Table S1: Summarizing table of the dependence of measured SP on the size and the height in the case of the P3HT and PDI singly or blended deposited on native SiO_x .

References

- (1) Nolde, F.; Qu, J. Q.; Kohl, C.; Pschirer, N. G.; Reuther, E.; Müllen, K. *Chem. Eur. J.* **2005**, *11*, 3959-3967.
- (2) Palermo, V.; Palma, M.; Samori, P. *Adv. Mater.* **2006**, *18*, 145-164.

- (3) Jacobs, H. O.; Leuchtmann, P.; Homan, O. J.; Stemmer, A. *J. Appl. Phys.* **1998**, *84*, 1168-1173.
- (4) Samorì, P.; Francke, V.; Mangel, T.; Müllen, K.; Rabe, J. P. *Optical Materials* **1998**, *9*, 390-393.
- (5) Liscio, A.; Palermo, V.; Gentilini, D.; Nolde, F.; Müllen, K.; Samorì, P. *Adv. Funct. Mater.* **2006**, *16*, 1407-1416.
- (6) Liscio, A.; Palermo, V.; Samorì, P. *in preparation* **2007**.

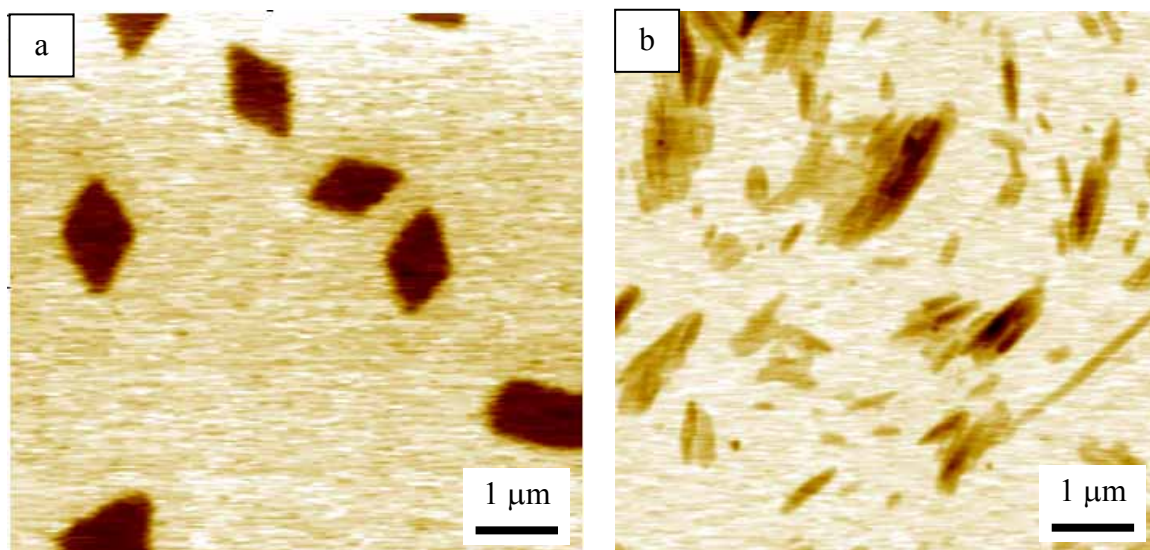


Figure S11: KPFM images of a) P3HT and b) PDI deposited on native SiO_x . P3HT aggregates in rhomboidal structures with lateral size of about $1 \mu\text{m}$ and possessing a SP of $-31 \pm 2 \text{ mV}$ with respect to that of the substrate. PDI aggregates into needle-like assemblies, which are preferentially aligned along their major axis (length) and pile-up forming 300 nm thick clusters. Single needles or small clusters formed only by aligned needles possess a $\text{SP} = -14 \pm 4 \text{ mV}$, while for higher clusters the SP decreases down to about -80 mV . The cross-talking between the topographic and potential signals can be neglected, and this effect can be ascribed (i) to the band bending of PDI when it is in contact with the substrate and (ii) to the averaging of the SP signal due to the effective volume of the sample which interacts with the tip. Z-scales: a) 40 mV and b) 90 mV .

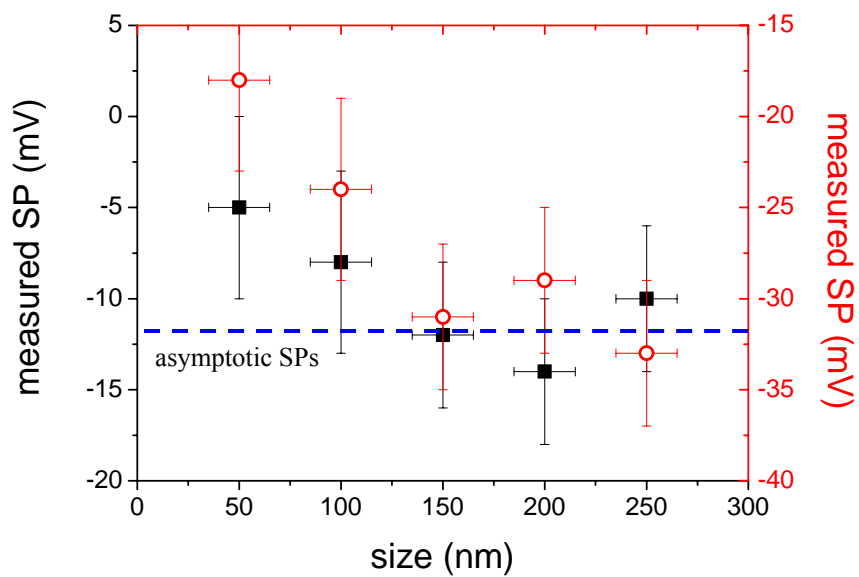


Figure SI2: Dependence of measured SP on the size (i.e. width) of the isolated PDI clusters adsorbed on native SiO_x estimated on illuminated samples (red open circles) and under dark (black squares). The SP values are displayed using the same potential range in the two axes which are shifted to align the two asymptotic SP values.

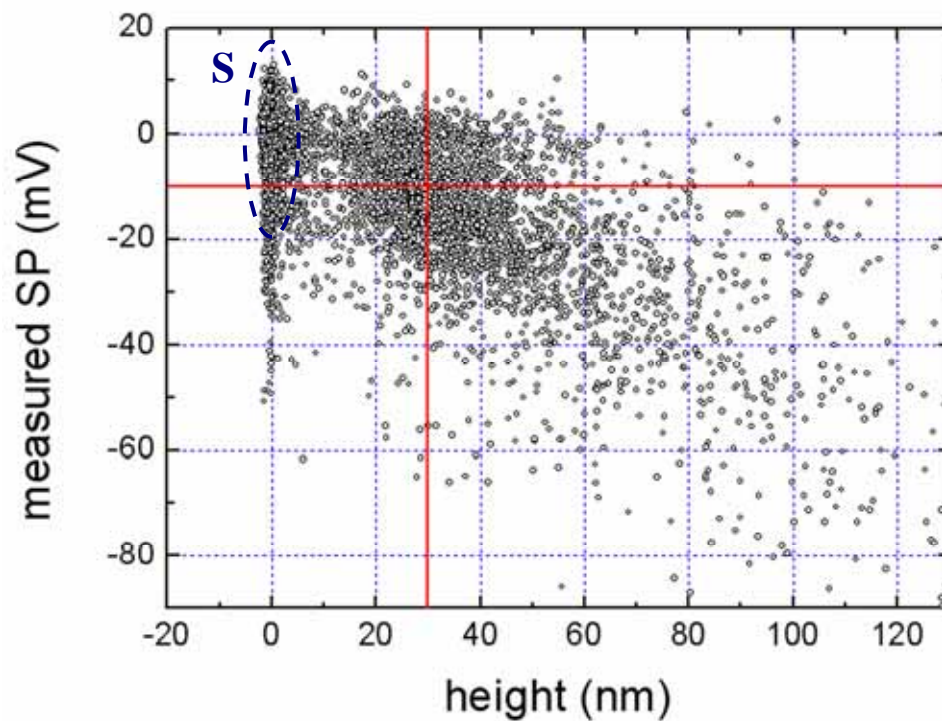


Figure SI3: Correlation plot of measured height values against the SP values of the PDI needle-like aggregates deposited on native SiO_x . In the graph are reported all the measured data. Both measured SP and height axes are shifted to set to corresponding values of the substrate (marked with S). The vertical and the horizontal red lines show the SP and the height of the PDI isolated clusters observed in P3HT:PDI blend when the sample is under dark.